

# Total-Internal-Reflection Fluorescence Microscope Characterization for Imaging-Fluorescence Correlation Spectroscopy

Student: Alon Shapiro

Supervisor: Prof. Paul Wiseman

Co-supervisor: Ahmad Mahmood, PhD Candidate

## Abstract

Quantitative fluorescence microscopy is an important tool in cell biology and biophysics as it allows the measurement of dynamic biological processes on micrometer scales in living cells. In this project, a protocol was produced for the purpose of determining the point spread function parameter (calibration) of a total internal reflection fluorescence microscope, which is required for the fitting of autocorrelation functions to the data, a key step in imaging fluorescence correlation spectroscopy, which is a powerful method for analysis of fluorescent signal fluctuations. Technical difficulties are discussed, and future steps are proposed to improve the calibration process.

## 1 Introduction

### 1.1 Fluorescence

Fluorescence is an atomic process in which an electron is promoted to a higher energy state by absorbing a photon (excitation, Spring, n.d.). After energy loss due to vibrational changes of the atom, the electron returns to its ground state while emitting a photon of lower energy (emission). This phenomenon occurs over a range of excitation and emission wavelengths which vary for different fluorescent species (Fig. 1).

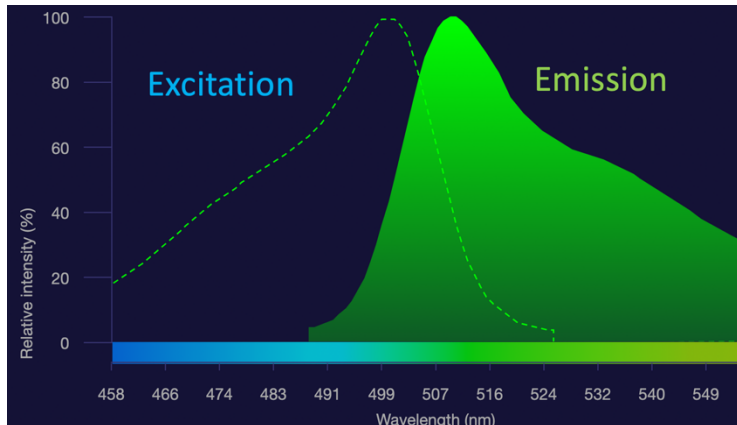


Figure 1. Excitation and emission spectra for the sample used in this project. Taken from ThermoFisher.

### 1.2 Diffusion

Brownian motion is the random movement of particles in a fluid on the microscopic scale, caused by thermal energy. When there exists a concentration gradient of some kind in a body of fluid, the gradient will undergo a process called diffusion as a result of the Brownian motion of the fluid. Diffusion means that particles move from an area of high concentration to an area

of lower concentration, reducing the gradient between different points in the fluid (Einstein 1905). Diffusion in one dimension can be described by the diffusion equation:

$$\frac{\partial C}{\partial t} = D \frac{\partial^2 C}{\partial x^2} \quad (1)$$

where  $C$  is the concentration at position  $x$  at time  $t$ , and  $D$  is the diffusion coefficient, which characterizes the time and length scale of the diffusion (Crank 1975).

The diffusion coefficient depends on the geometry of the diffusing particles and on the properties of the medium in which the diffusion is occurring. For a spherical particle of radius  $r$ , diffusing through a liquid of viscosity  $\eta$  at temperature  $T$ , the diffusion coefficient  $D$  is given by the Stokes-Einstein equation:

$$D = \frac{k_b T}{6\pi\eta r} \quad (2)$$

where  $k_b$  is Boltzmann's constant.

### 1.3 Fluorescence Correlation Spectroscopy and the Autocorrelation Function

Fluorescence correlation spectroscopy (FCS) is a biophysical method based on measurement and analysis of fluctuations in fluorescence intensity of a sample within a small volume defined by a tightly focused laser beam. In the context of biophysics, it allows diffusion coefficients for particles and molecules to be measured from fluctuations caused by Brownian motion (Milon et al. 2002). An intensity fluctuation autocorrelation function (ACF) can be generated through FCS which measures the temporal self-similarity of the fluorescence signal of the sample, and with prior knowledge of the underlying physical process allows the data to be fitted to a theoretical model, from which information about the system can be acquired (Ng et al. 2015). If we define the fluorescence signal collected from the beam focus at the sample as  $F(t)$  as a function of time with average value  $\langle F \rangle$ , the normalized intensity fluctuation ACF,  $G(\tau)$  can be defined as follows:

$$G(\tau) = \frac{\langle \delta F(t) \cdot \delta F(t + \tau) \rangle}{\langle F(t) \rangle^2} \quad (3)$$

where the signal fluctuations are defined as  $\delta F(t) = F(t) - \langle F(t) \rangle$  and the angular brackets in the numerator signify the mathematical correlation operation.

Two important dynamical parameters which can be obtained from the ACF are the average number of particles that diffuse in and out of the observation volume, which is inversely

proportional to the amplitude of  $G(\tau)$ , and the diffusion coefficient of the system which is encoded in the decay rate of the ACF for particles obeying Poisson statistics (see Fig. 2).

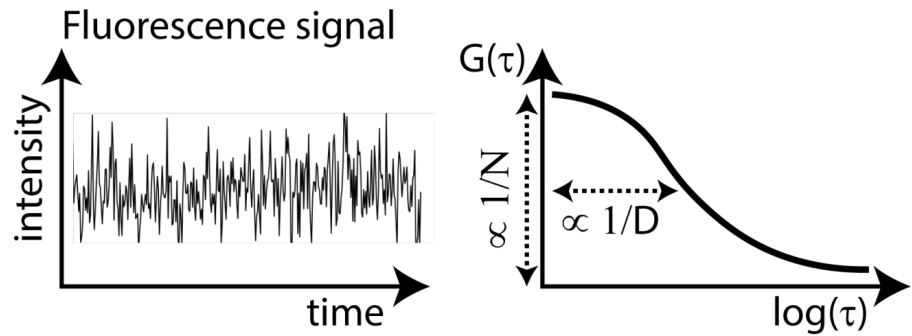


Figure 2. On the left, fluorescence signal along time. On the right, an ACF. The sample concentration  $N$  is given by the amplitude of the ACF, and the diffusion coefficient  $D$  of the sample is given by the decay rate of the ACF. Taken from Mahmood 2020.

Traditionally, FCS involves measurements from a single spatial ‘point’ in the sample over time (see section 1.5). This constrains the power of FCS in biological imaging, but advancements such as TIRF (see section 1.7) find ways to overcome this constraint.

#### 1.4 The Point Spread Function

Many modern fluorescence microscopes involve capturing the sample image with a camera. The aperture of the objective lens causes diffraction of light, an effect that is described by the point spread function (PSF) of the optical setup (Sankaran et al. 2013). Therefore, the image that falls on the camera sensor is a convolution of the light emitted from the fluorescent molecules in the sample and the PSF, which causes the final image to appear fuzzy due to light diffraction, illustrated in figure 3 (Sankaran et al. 2013). The PSF has two components (see Fig. 3), the lateral  $w_{xy}$  component which describes the spread in the lateral plane (laterally to the direction in which emitted fluorescent light travels toward the detector), and  $w_z$  which describes spread in the vertical direction (in the same direction as the emitted fluorescent light travels toward the detector).

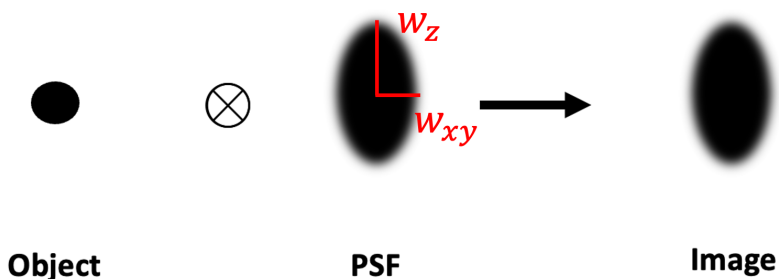


Figure 3. The image that falls on the camera sensor is a convolution of the object and the PSF of the microscope objective lens. To help with visualization of the PSF effect, the figure illustrates an x-z slice of the PSF.

## **1.5 Confocal FCS**

The most conventional FCS setup involves using a confocal microscope, which uses lenses to focus a laser at a single point of the sample, creating a roughly spherical observation volume of a few femtoliters (Mahmood 2020). The small observation volume poses multiple limitations. First, many biological processes occur over much larger volumes, which means that a small observation volume heavily limits understanding of the whole system (Guo et al. 2014). Second, diffusion times in biological systems are often long, which means that acquiring sufficient data from a small volume takes a long time (Sankaran et al. 2009).

## **1.6 Imaging FCS**

Imaging FCS (ImFCS) provides a solution to both these problems. By combining a microscope illumination scheme which allows a whole plane of the sample to be viewed at once together with a fast camera sensor, FCS can be done at multiple spatial points (spatial multiplexing) at the same time (Ng et al. 2015). This allows for much faster data acquisition. Moreover, it allows for a much larger observation volume (which actually becomes an observation area), which allows for biological processes that occur over larger areas to be properly observed (Guo et al. 2014). This solves the concerns that were raised with confocal FCS, but requires a new approach to how the imaging is performed.

## **1.7 Total Internal Reflection Fluorescence Microscopy**

Total internal reflection fluorescence (TIRF) microscopy employs the evanescent wave of light produced at the objective lens of a microscope when the illumination laser is directed at a critical angle of incidence, thus generating total internal reflection (see Fig. 4). The exponentially decaying evanescent wave restricts excitation of fluorescence to fluorophores (fluorescent particles) found close to the glass slide surface (about 100 nm penetration depth, Bag et al. 2012). This creates a very thin observation layer due to the rapid decay of the evanescent tail and allows an approximated flat 2-dimensional area to be observed, which makes TIRF an excellent technique for lipid bilayer and cell membrane observations of adherent cells (Bag et al. 2012). When combined with a fast camera sensor, each pixel acts as a pinhole resembling a confocal microscope observation volume, which allows for thousands of ACF's to be computed after just one observation time window over all the pixels (Bag et al. 2012).

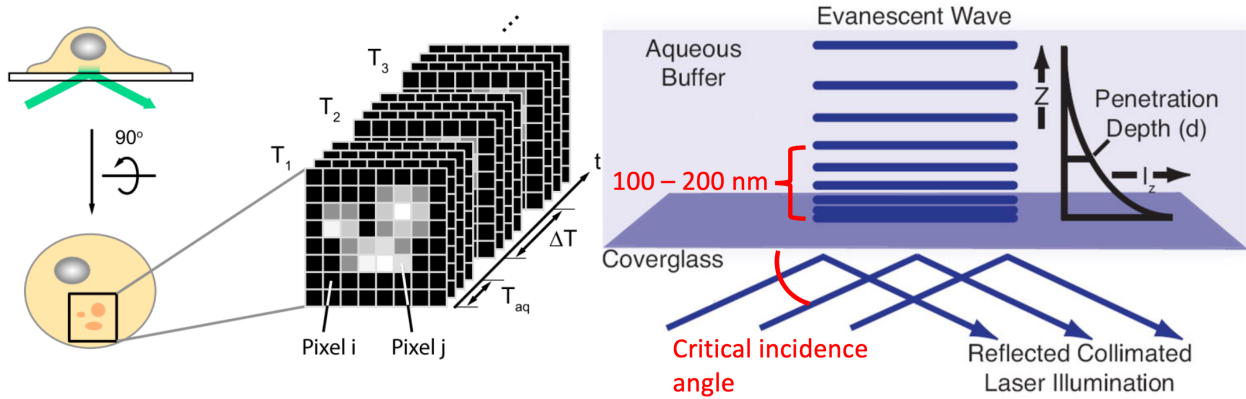


Figure 4. On the left, illustration of a live cell being imaged on a TIRF microscope. The images are collected and stored as an image stack (movie) which then allows each pixel to be analyzed as an observation point (taken from Kannan et al. 2007). On the right, an evanescent boundary wave forms at the border of the glass slide and the sample (taken from Fish, 2009).

## 1.8 ImFCS on a TIRF microscope

When ImFCS is performed with a TIRF microscope, the PSF only retains the lateral component  $w_{xy}$  (Bag 2012). This happens because the sample illumination is restricted to a very thin plane closest to the boundary of the glass slide. The PSF is then used to fit the ACF function  $g(\tau)$  to the data with the following fitting function:

$$g(\tau) = G_\infty + \frac{1}{N/A_{\text{eff}}} \cdot \frac{1}{a^2} \cdot \sum_{i=1}^3 \rho_i \cdot \left[ \text{erf} \left( \frac{a}{\sqrt{4D_i\tau + w_{xy}^2}} \right) + \frac{\sqrt{4D_i\tau + w_{xy}^2}}{\sqrt{\pi} \cdot a} \cdot \left[ \exp \left( -\frac{a^2}{4D_i\tau + w_{xy}^2} \right) - 1 \right] \right]^2 \quad (3)$$

where  $G_\infty$  is a constant offset,  $N$  is the number of particles in the observation area,  $A_{\text{eff}}$  is the effective lateral focal area,  $a$  is the width of the pixel in the image plane,  $D$  is the diffusion coefficient of the particles, and  $\tau$  is the correlation time (time-lag). The subscript  $i$  is used when there are multiple species diffusing in the sample, and  $\rho_i$  is the fraction of the  $i$ 'th component (Bag 2012). For the purposes of this project, both  $i$  and  $\rho_i$  were equal to 1.

## 1.9 Project motivation

TIRF microscopy thus permits much faster data acquisition for systems such as lipid bilayers which allow membrane dynamics and transmembrane behaviour to be studied in living cells (Kannan et al. 2007). It is thus a valuable tool for a biophysics lab. As such, this project seeks to standardize the procedures involved in using the TIRF microscope in our lab and make it efficient and smooth, which will help future research projects acquire more data at a faster rate and improve the methodology involved.

## **2 Project goals**

### **2.1 Calibration**

The calibration procedure is a structured method of determining the PSF of the microscope, which is required for quantitative analysis of acquired data. To determine the PSF, the calibration procedure described in the methods section will be followed (see section 3.2.1).

### **2.2 Validation**

After the PSF is determined, measurements taken with the TIRF microscope should be validated against measurements obtained for the same sample with confocal FCS. Concentration measurements of different samples would be compared from both microscopes to determine whether they are in agreement with each other. Then, the measured diffusion coefficients would be compared for all samples to determine whether both microscopes agree.

However, due to some difficulties and delays, the validation was not performed.

### **2.3 Protocol write up**

A detailed protocol has been written up as part of the methods section of this final report in order to outline all the procedures and actions which have to be performed during the calibration process, including sample preparation and imaging, and data analysis with the software QuickFit 3.0.

## **3 Methods**

### **3.1 Imaging**

#### **3.1.1 Sample preparation**

The sample chosen for the calibration was 100 nm and 200 nm fluorescent beads produced by ThermoFisher Scientific. They were chosen since their diffusion coefficients can be determined theoretically using the Stokes-Einstein equation. Both bead sizes are excited by 505 nm light and emit 515 nm light (see Fig. 1 for spectra).

A detergent (Tween20) was used to prevent bead immobilization on the glass slide surface and to increase the viscosity of the solution.

Following is a brief description of the sample preparation. First, two pieces of coverslip-tape are placed at a distance of about 1.5 cm apart on the glass slide. Both glass slide and coverslip are put under gentle pressurized air flow to remove any dust, and the coverslip is placed on top of the coverslip-tape, and gentle pressure is applied to the sides of the coverslip to make it adhere to the tape. The glass slide is placed on a hotplate for 10 minutes until the tape is partially molten to allow stronger adhesion of the coverslip. Using a micropipette, 50  $\mu\text{L}$  of the sample is placed between the coverslip and the slide and allowed to move into the space between them.

Nail polish is then used to seal the coverslip from all sides. The glass slide is labelled with the sample type and concentration using a sharpie pen. The slide is covered by aluminum foil for 10 minutes to let the nail polish dry.

### **3.1.2 Sample placement on microscope**

To place the slide on the microscope stage safely, the following short procedure should be followed. Move the objective lens to the highest position and using a piece of lens paper and some ethanol, gently wipe the objective lens to clean it. Place one drop of immersion oil on the lens and move it to the lowest position using the focus knob. Place the slide on the stage and clamp it. Slowly move the objective lens toward the glass slide until the oil makes contact with it and spreads between the slide and the lens.

### **3.1.3 Instrument set up**

The TIRF microscopy was done on an Olympus IX71 microscope and ANDOR Sona-11 (22 mm) camera with a fast 1400x1400 pixels ( $11 \mu\text{m} \times 11 \mu\text{m}$  pixel size) EMCCD camera sensor. The imaging with the TIRF microscope currently requires the operation of 3 programs: Micro-Manager 2.0.0 (MM2) for the camera, Labview 'TIRF' for the laser, and Kinesis for the motor control. Following is the procedure for preparing the hardware and software for imaging. Turn on both computers and wait for them to load. Then, flip the left laser-box switch on and wait for the laser-box to initialize. Turn the motor on. Switch the safety key on the laser-box to the 'on' position. Open the 3 programs described above on the TIRF computer, found on the desktop. In Kinesis, click the 'Home' button to set the motor to its initial position, and then move it to around 17.7 - 17.9 mm. In Labview, click the 'Start' button, and skip all error messages (those are raised since not all defined plugins are found, but those are not needed for our purpose). Set the 488 nm slide to 5-10 % power and click the 'OFF' button to turn on the laser. In Micro-Manager, set exposure to 1 ms (or desired exposure), and click on 'Live' button to see live feed from camera. Click on 'Auto once' to adjust the brightness of the image. Using the focus knob on the microscope, slowly bring the objective lens up toward the sample until beads are visible. Keep re-adjusting the brightness repeatedly by clicking the 'Auto once' button every few seconds.

Bit depth of acquisition can be changed by going to Plugins > Device Property Browser (Note: even though acquisition can be performed in 12-bits, the image stack is still saved as a 16-bit image, since there is no 12-bit format for images. However, 12-bit acquisition allows for a much greater frame rate).

To change the ROI, draw a square in the live image window of the desired ROI. The coordinates can be seen in the ImageJ window that opens with the MM2. The coordinates are defined such that the top left corner is the origin, and the values increase downward and to the right. To apply the new ROI, click button 1 in the MM2 main window (see Fig. A1). Button 2 can be used

to re-set the ROI to the maximal size. Frame rate varies continuously with the ROI size, such that any decrease in ROI increases frame rate. To optimize image acquisition time, choose ROI's that are symmetrical around the horizontal axis at the mid-point of the camera sensor (symmetrical around the 'x axis'). To record a video, click on the 'Multi-D Acq.' button in the main MM2 window (button 3 in Fig. A1). Set the number of frames in the 'count' field. For fastest acquisition, set the 'Interval' field to zero (time between frames). Choose the desired directory to save the file and name it appropriately. Click 'Acquire!' to start recording the images (make sure the lights in the room are turned off before starting the recording).

### 3.1.4 TIRF identification

Once the microscope focus and motor distance are set such that bead diffusion is visible, the critical incidence angle has to be found. First, the glass slide-sample boundary has to be located by finding the depth where immobilized beads are visible by adjusting the microscope focus knob. Next, the motor has to be 'Jogged' around until the image appears as TIRF rather than widefield, and any artifacts (such as the big circular artifact which can be observed at the biggest ROI mode) in the image disappear. The image brightness and microscope focus have to be adjusted repeatedly during the motor jogging. TIRF is very distinct from widefield- in TIRF, lateral movement of beads is not observable, but rather they appear to be twinkling, whereas in widefield the path of the beads is visible (see table 1 for all differences and Fig. 5 for some visual differences). Lastly, when the appropriate motor distance is located for TIRF and the image is in focus, very small movements of the focus knob will cause a rapid de-focusing of the image, compared to widefield.

Characteristic	TIRF	Widefield
Bead path	No path is visible	Directionality of bead diffusion path is discernible
Bead appearance	Completely circular, twinkling	Slightly ellipsoidal, brightness changes gradually as bead diffuses into and out of the evanescent wave
Out-of-focus beads	Not visible	Visible and faint compared to beads closer to surface
De-focusing by microscope knob	Very rapid, appears as bright rings around bead	Gradual, appears as a fuzzy circle
Image contrast	High, no background noise is visible	Low, background noise and out-of-focus beads visible

Table 1. Main differences between TIRF and widefield images to look for.

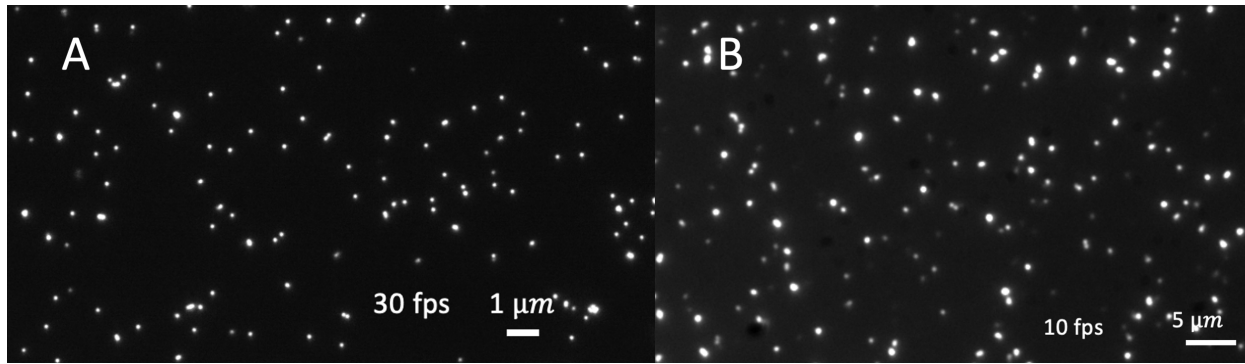


Figure 5. Image of 100 nm beads taken in A) TIRF and B) widefield regimes. The TIRF image has higher contrast and much less visibility of beads diffusing farther from glass slide compared to widefield.

### 3.1.5 Imaging metadata

After image acquisition, Micro-Manager generates a metadata file (with name '[NAME]\_MMStack\_Default\_metadata') which records all the imaging parameters such as the ROI size, bit depth (12 or 16), number of frames, total acquisition time, frame rate, exposure time, etc., which can be consulted during the data analysis for the required imaging settings.

## 3.2 Data analysis

### 3.2.1 General calibration procedure

The general calibration procedure is as follows (Bag 2012). After acquiring a TIRF image stack for a single diffusing species, a range of reasonable guesses for the PSF is inputted into the analysis software (see section 3.2.2). These PSF parameters are used to fit the ACF's and determine the diffusion coefficient value of the sample. At increased bin sizes (also referred to as pixel size), the ACF fitting becomes independent of the PSF parameter, making all the D values of the different PSF guesses to converge (Fig. 6A, first step of calibration). The average D value at the highest binning is taken as the reference D value ( $D_{ref}$ ). The ACF's are then recalculated with the  $D_{ref}$ , while varying the PSF parameter within the range of the original guesses (Fig. 6B, second step of calibration). The PSF parameter at the smallest binning size is taken as the true PSF parameter, which can then be used for ACF fitting and future analysis.

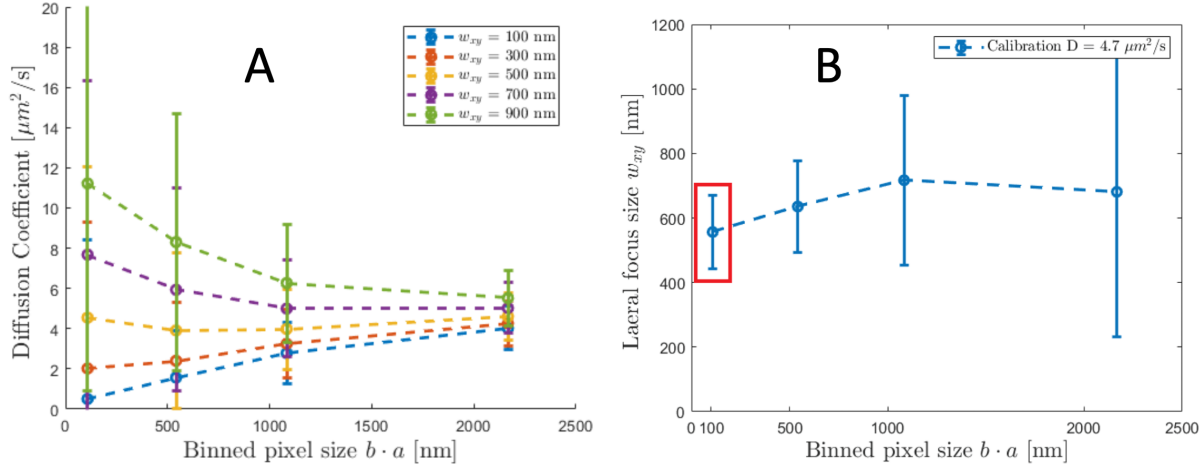


Figure 6. Plots produced by the two steps of the calibration process. A) Diffusion coefficients vs. pixel size plot,  $D$  at largest pixel size is the reference  $D$ . B) PSF vs. pixel size. PSF at smallest pixel size is the true PSF. Taken from Mahmood 2020.

A TIRF image of bead diffusion is required for PSF calibration. With our camera, an ROI of (70 x 70) up to (90 x 90) pixels is sufficient for binning, with smaller ROI's more favourable due to increased time resolution, one of the main constraints on the calibration accuracy (Sankaran 2013). Accuracy depends on the ratio of frame time  $\Delta\tau$  to diffusion time  $\tau_d$  (time it takes particle to diffuse over the area of a pixel)  $\frac{\Delta\tau}{\tau_d}$ , where  $\tau_d = \frac{A_{eff}}{4D}$ , and  $A_{eff}$  is the pixel area.

Therefore, slowing the sample diffusion can also provide advantages to accuracy. This can be done by increasing the viscosity of the solution by adding a detergent such as Tween20 or sucrose, or by using bigger bead species (such as 200 nm beads rather than 100 nm). To increase the precision of the calibration, the acquisition time has to be increased by taking more frames (see Fig. 7). With our camera pixel size, there is a big improvement in accuracy going from 50,000 frames to 100,000 frames, however the accuracy is still not good (up to 50% error in  $D$ ). Due to the constraints in the analysis software used (see section 3.2.2), images with more than 100,000 frames are not accepted as the file size exceeds the accepted size limit.

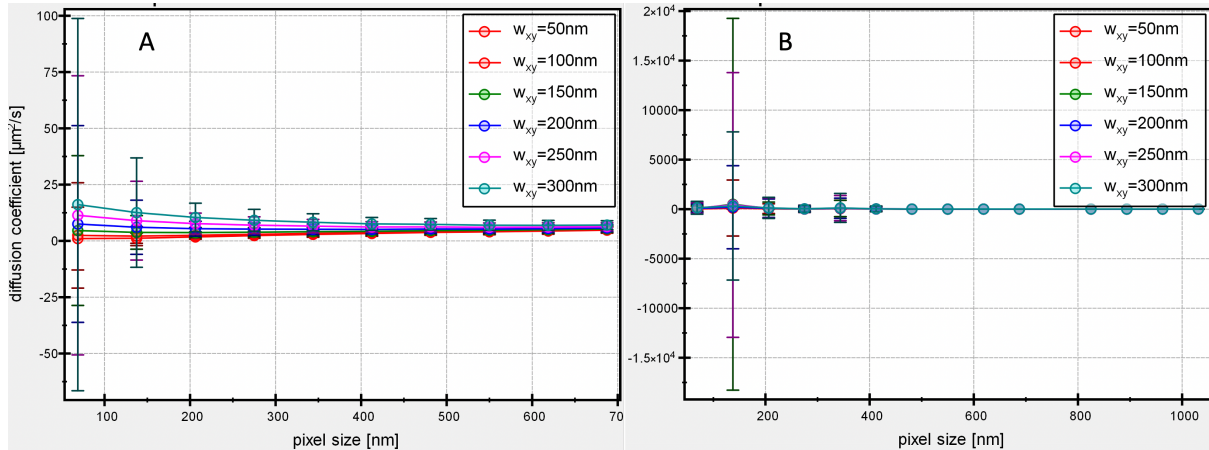


Fig. 7. Diffusion coefficients vs. pixel size plot. Error bars on  $D$  during first step of calibration for 200 nm beads diffusion in 0.5% Tween20 solution. A) Image stack of 100,000 frames. B) Image stack of 50,000 frames. A visual inspection shows the massive improvement in precision for analysis with more frames.

If after the first step of the calibration a trend is observed in the convergence of the D values (increasing or decreasing, see Fig. 8A), this is an indication that the true PSF parameter does not lie within the range of the initial PSF guesses. The step has to be repeated and the PSF parameter guesses have to be adjusted. This has to be repeated iteratively until the D convergence has no obvious trend (see Fig. 8B).

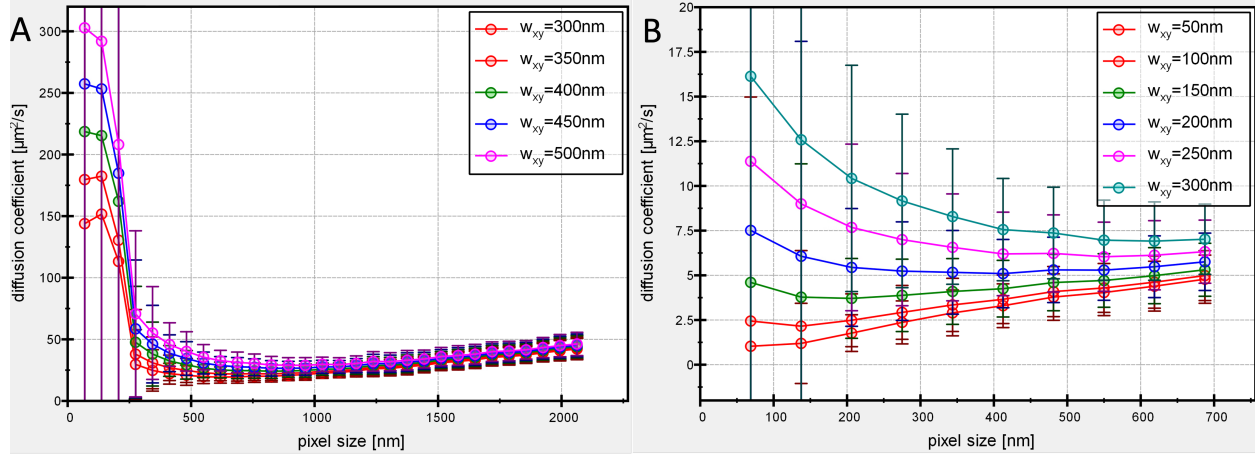


Fig. 8. Plot of D against pixel size. A) Initial PSF guesses range from 300 nm to 500 nm, with the true PSF (around 230 nm) outside the guess range. A decreasing trend until 700 nm pixel size and then an increasing trend can be clearly observed. Since 60,000 frames were used, the accuracy is very low. Pixels were binned 30 times. B) Initial PSF guesses range from 50 nm to 300 nm, with the true PSF lying within the guess range. There is a horizontal convergence toward  $D_{ref}$  with no clear trend. An image stack of 100,000 frames was used, leading to improved precision. Pixels were binned 10 times.

At larger binning sizes, signal to noise ratio decreases and makes statistics unreliable (Bag 2012). This can be observed in Fig. 8, A where beyond a pixel size of about 1000 nm, an increasing trend is present, which should not be there. Therefore, binning should be limited to a reasonable number of steps which can be determined empirically (Bag 2012). For our setup, binnings of up to 15 steps produce reliable convergence and estimate for  $D_{ref}$  (see Fig. 8B).

### 3.2.2 Calibration with QuickFit 3.0

The above calibration procedure can be performed in QuickFit 3.0 (QF), which was the chosen analysis software for this project. After opening the software, click on 'Data Items > Insert Raw Data > imFCS: Imaging FCS > imaging FCS Correlation Wizard (don't add fits) ...'. The 'Imaging FCS/FCCS Wizard' will come up (see Fig. A2). Choose 'imFCS focus volume calibration' and click 'Next'. Choose the image stack for the calibration and click 'Next'. (Note: if software takes more than a few minutes to load, it is likely the file exceeds the size limit of 2 GB. The software has to be closed and re-launched and a smaller file must be used. One option is to crop the image stack with ImageJ to reduce its size). The 'image stack properties' window will come up (see Fig. A3). Make sure that the correct file was loaded by looking at the image and the number of frames. Click on 'calculate ...' to calculate the pixel size in the image space given the camera

pixel size and the objective magnification, then click 'OK' to apply the calculated pixel size. Input the frame time that was used in microseconds. This is the inverse of the frame rate, which can be found in the imaging metadata file. The frame rate value has to be inverted (divide 1 by it), and then multiplied by  $10^6 \frac{s}{\mu s}$  to convert it from seconds to microseconds. Click 'Next'. Make sure 'TIRF microscopy' is chosen as the option for 'Microscopy Technique' and click 'Next'. The 'Background and Bleach Correction Setting' window will come up (see Fig. A4).

Load a background noise file if desired by choosing 'remove background image & offset' in the first dropdown menu and navigate to the background noise image stack in the second line. Bleach correction should not be used for bead samples.

Note: When I was subtracting background noise, I would get overflow of values (beads become dark and surroundings become white).

Click 'Next'. The 'Setup Calibration' window will come up (see Fig. A5). Verify the image is not overflowing if background was subtracted. Unless otherwise desired, leave the max lag-time and number of correlated segments as default. Input the expected PSF parameter. For our TIRF setup, this is around 250 nm. Choose how many PSF parameters around the expected value to use for the calibration, and the step size between them (5 initial guesses distributed around the expected value with step size of 50 nm yields good results). Lastly, choose the maximal binning size. For our setup, this should be between 10 and 15 pixels. Click 'Next' and wait for the ACF curves to be calculated. The 'maximal parallel jobs' number on the top right can be increased to around 5 to speed up the process. Click 'Next' and then 'Finish'. The software will now load the calculated ACF's and the user will be prompted to save the project. This is highly recommended since QF frequently crashes unexpectedly. Once the loading is done, the ImFCS calibration window will come up (see Fig. A6). The calibration can now be started by clicking on the 'run step 2' button. This will calculate D values with all the initial PSF guesses. When this is done, 'run step 3' will plot the D value vs. pixel size plot in the top figure. A pop-up window will come up asking for the pixel size at which the  $D_{ref}$  should be calculated. Unless otherwise desired, choose the largest pixel size. Next, 'run step 4' will use the determined  $D_{ref}$  to re-fit the ACF's with varying  $w_{xy}$  values. Lastly, 'run step 5' will plot the calculated  $w_{xy}$  values against pixel size. The PSF parameter at the smallest pixel size is the true PSF parameter.

### 3.2.3 ACF fitting with QuickFit 3.0

After calibration (or if PSP parameter has been previously determined), the ACF can be fitted to data. After opening the software, click on 'Data Items > Insert Raw Data > imFCS: Imaging FCS > imaging FCS Correlation Wizard (don't add fits) ...'. Choose 'imFCS / imFCCS evaluation'. The same sequence of windows as for the calibration will follow (see section 3.2.1). When the 'Microscope type' window is reached (see Fig. A7), the known PSF parameter should be specified. Click 'Next' through all the following windows and then 'Finish'. The calculated ACF's

can now be found in the main software window (see Fig. A8). Double click it to open the ACF window. The ACF's can be evaluated visually in the 'Correlation Curves' tab. In order to fit the data to the ACF function, in the main software window, click on 'Data Items > Insert Evaluation > imFCS Curve Fitting'. The 'imFCS Fit' window will open (see Fig. A9).

Choose 'TIR-FCS (camera): 2D Normal Diffusion (rect. pixel, 1/e^2 radii)' from the 'Fit Model' dropdown menu (see Fig. A9, arrow 1). Next, click on 'Fit Current' (small red rectangle on right) to fit the ACF for the current pixel. The fit for the current pixel can be evaluated visually from the figure and by looking at the D value that is determined by the fitting ( $D_1$ , see Fig. A9, arrow 2). If the D value matches the expected value from theory (for spherical beads), the fitting parameters can be set as the initial guess for the fitting parameters for all the pixels by clicking on 'Copy to Initial'. Then, clicking on 'Fit All pixels, this file (newMT)' will start the fitting of the ACF to all the pixels in the current open file (see Fig. A9, arrow 2).

Once the fitting is done, the fitted parameters can be evaluated. Navigate back to the main software window and double click the ACF entry in the 'Raw Data Records' section (see Fig. A8). The fitting evaluation window will open (see Fig. A10).

Choose 'imFCS Fit ...' in the 'result set' dropdown menu to display the fitting results (see Fig. A10, arrow 1). Different fitting parameters can be chosen for evaluation in the 'parameter' dropdown menu (see Fig. A10, arrow 2). Lastly, fitting parameters can be evaluated in the 'Images/Data', 'Histograms', and 'Correlations' tabs (see Fig. A10, arrow 3).

## 4 Calibration Results

Results have been obtained for various bead concentrations (0.02%, 0.2%, 1%) and sizes (100 nm, 200 nm), and in different solutions (water, water with 0.5% Tween20), but for brevity, the results for 200 nm beads of concentration 0.2% diffusing in 0.5% Tween20 solution will be presented here (see Fig. 9, Fig. 10). The imaging was done over an ROI of 90x90 pixels at 1 ms exposure, with 100,000 frames, at a frame rate of  $994.5\text{ s}^{-1}$ .

Initial PSF parameter guesses were over the range of 50 nm to 300 nm, at 50 nm jumps (see Fig. 10). The  $D_{ref}$  value was determined to be  $(5.7 \pm 0.9)\text{ nm}$ . PSF parameter at smallest binning size was determined to be  $(221 \pm 60)\text{ nm}$ , in agreement with the expected value of about 230 nm.

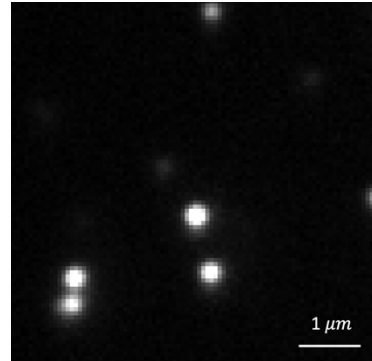


Figure 9. Beads of 200 nm radius at 0.2% concentration diffusing in 0.5% Tween20 solution.

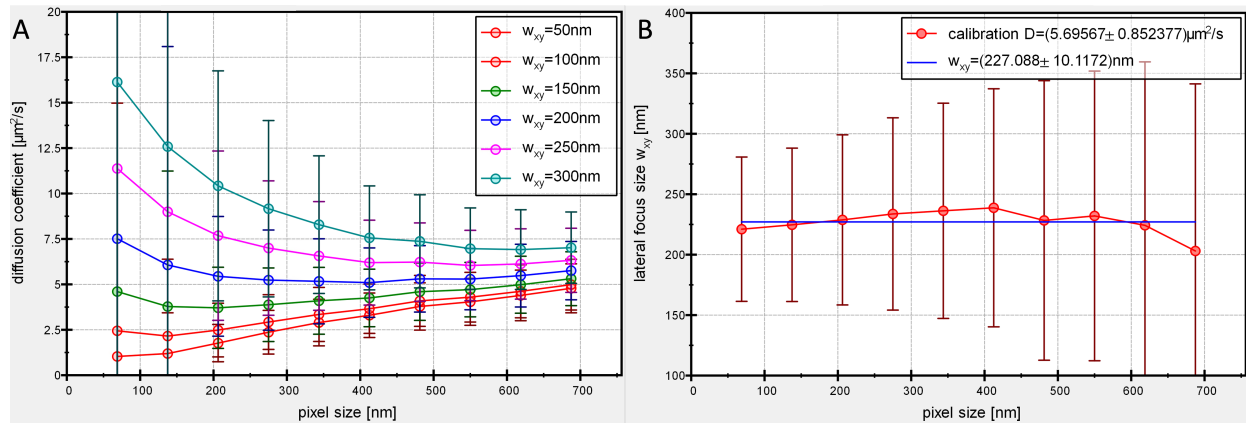


Figure 10. Calibration results for 200 nm beads in 0.5% Tween20 solution. A) Diffusion coefficient values vs. pixel size plot displays horizontal convergence with no obvious trend. B) PSF parameter vs. pixel size. Value at smallest pixel size is  $(221 \pm 60)$  nm.

## 5 Discussion

### 5.1 Difficulties and Challenges

Multiple difficulties were encountered during the technical execution of the project. For example, the TIRF microscope that was used can either produce TIRF images or widefield images (see section 3.1.4). However, the differences between the two types of images are very subtle and are not noticeable to the unexperienced eye. A lot of data (>50 GB of data) that was thought to be TIRF was collected and used for the calibration, which would fail as the calibration is not designed for widefield images. A lot of time was spent trying to troubleshoot the calibration and determine why the wrong results are being produced, while the simple fact that the acquired images were not actually TIRF images was overlooked. Another source of much delay was the wrong assumed expected PSF value. It had been assumed for a long time that the true PSF lies between 300 nm and 500 nm. When these guesses were used for the calibration, they were producing unexpected results. The fact that the expected PSF lies outside of this range, and the fact that for the calibration to be successful the true PSF must lie within the guess range, were discovered at a much later point in time, after many failed troubleshooting attempts.

Another big challenge in the project was the wet lab component. Some dilution calculations and sample solution preparation of varying concentrations and compositions were required at a certain point of the project. These are basic wet lab procedures. However, for individuals who have never received any wet lab training and never worked in a wet lab, these basic procedures were completely foreign and required quite some time to figure out.

Together, these difficulties and challenges caused delays in the progression of the project.

## 5.2 Calibration results and Future steps

After overcoming the challenges outlined in the previous section, adequate calibration results were successfully produced with 200 nm beads in 0.5% Tween20 solution (see Fig. 10). Despite a much less pronounced trend in the diffusion coefficient vs. pixel size plot, the convergence still appears to be slightly directed in an upward trajectory. Due to the big error bars compared to the determined values, it is not clear whether this effect is caused due to the uncertainty (due to a limited number of frames), or due to some other unknown cause. To determine whether the issue is caused by the low number of frames, an image stack with many more frames should be acquired for the same sample (around 200,000 to 300,000 frames), and the stack should be calibrated using a different program such as ImageJ ImFCS plugin (the file size limit for this program is 98 GB, which means it would be able to load and process much bigger files than QF). The reason this hasn't been tried is because the availability of an alternative ImFCS calibration software was only discovered at a very late point in the project.

The  $D_{ref}$  value determined by the calibration ( $(5.7 \pm 0.9) \mu\text{m}^2/\text{s}$ ) is still much bigger than what is expected, which should be closer to  $1 \mu\text{m}^2/\text{s}$ . This means that the accuracy of the calibration is not good enough. ImFCS accuracy is primarily determined by the time resolution of the acquisition, which can be improved by either slowing down the system dynamics or speeding up the frame rate. The frame rate of the camera heavily depends on the ROI of acquisition and rises rapidly with decreasing ROI size. ROI sizes of 120 x 120 pixels and 90 x 90 pixels were used exclusively for image acquisition during this project, since it was determined that up to 30 binning steps would be required for the ACF to become reliably independent of the PSF. However, Bag et al. (2012) determined that complete convergence of the diffusion coefficient values in the first step of calibration is not required, as the signal becomes unreliable at big binning steps. Instead, as long as there is a decent convergence (visually) at lower number of binning steps,  $D_{ref}$  can be determined and used for the second step of the calibration. Therefore, a much smaller ROI should be used in the future in order to increase the frame rate of the camera, since an ROI of 90 x 90 pixels does not provide any advantages for the binning. A sufficient frame rate is expected to be achieved by reducing the ROI to around 60 X 60 pixels, while still allowing for enough binning steps. Despite an inaccurate  $D_{ref}$  value, the PSF parameter determined by the second step of the calibration at the smallest binning is within agreement with the expected value ( $(221 \pm 60) \text{ nm}$ ), albeit with a big uncertainty. Following the proposed future steps listed above should improve the accuracy and precision of both determined  $D_{ref}$  and the PSF parameter values.

After successful calibration with 200 nm beads, the calibration should also be performed with the 100 nm beads to evaluate the effect of the imaged bead size on the calibration. It is expected that calibration with a bigger bead size would yield a larger PSF parameter (due to the 'object function', which depends on the size of the imaged object). Thus, aggregating the determined PSF parameter values with various bead sizes, will allow extrapolation of the PSF

value to a bead radius on 0 nm, at which point a superior estimation of the true PSF parameter is expected.

Lastly, the validation of the TIRF microscope against either confocal FCS or ICS should be performed to benchmark ImFCS on the TIRF microscope.

## 6 Conclusions

Imaging FCS on a TIRF microscope provides a powerful tool for vast data acquisition at high speeds and allows for the whole biological context to be captured from a given sample. However, knowledge of the PSF of the microscope is required for the analysis of this data for the ACF fitting, which can be determined empirically through the calibration process. The calibration process for a TIRF microscope is sensitive to the choice of sample and to the image acquisition settings which are used. With an iterative process of varying these settings and the initial PSF parameter guesses, calibration can produce reliable results. Other than determining many technical aspects relating to optimizing calibration, key future steps were summarized to improve the calibration results and include using a smaller ROI to increase the time resolution of acquisition and using an alternative analysis program which is better fitted for calibration of our existing set up.

## References

Milon, Séverine & Hovius, Ruud & Vogel, H & Wohland, Thorsten. (2003). Factors influencing fluorescence correlation spectroscopy measurements on membranes: Simulations and experiments. *Chemical Physics*. 288. 171–186. 10.1016/S0301-0104(03)00018-1

Ng, X. W., Bag, N., & Wohland, T. (2015). Characterization of Lipid and Cell Membrane Organization by the Fluorescence Correlation Spectroscopy Diffusion Law. *Chimia*, 69(3), 112–119. <https://doi.org/10.2533/chimia.2015.112>

Mahmood, M.A. (2020). Characterizing a single plane illumination microscope for imaging fluorescence correlation spectroscopy. McMaster University – Department of Physics and Astronomy. URI: <http://hdl.handle.net/11375/26128>

Sankaran, J., Bag, N., Kraut, R. S., & Wohland, T. (2013). Accuracy and precision in camera-based fluorescence correlation spectroscopy measurements. *Analytical chemistry*, 85(8), 3948–3954. <https://doi.org/10.1021/ac303485t>

Guo, S. M., Bag, N., Mishra, A., Wohland, T., & Bathe, M. (2014). Bayesian total internal reflection fluorescence correlation spectroscopy reveals hIAPP-induced plasma membrane domain organization in live cells. *Biophysical journal*, 106(1), 190–200. <https://doi.org/10.1016/j.bpj.2013.11.4458>

Sankaran, J., Manna, M., Guo, L., Kraut, R., & Wohland, T. (2009). Diffusion, transport, and cell membrane organization investigated by imaging fluorescence cross-correlation spectroscopy. *Biophysical journal*, 97(9), 2630–2639. <https://doi.org/10.1016/j.bpj.2009.08.025>

Bag, N., Sankaran, J., Paul, A., Kraut, R.S. and Wohland, T. (2012), Calibration and Limits of Camera-Based Fluorescence Correlation Spectroscopy: A Supported Lipid Bilayer Study. *ChemPhysChem*, 13: 2784-2794. <https://doi.org/10.1002/cphc.201200032>

Kannan, B.S., Guo, L., Sudhaharan, T., Ahmed, S., Maruyama, I., & Wohland, T. (2007). Spatially resolved total internal reflection fluorescence correlation microscopy using an electron multiplying charge-coupled device camera. *Analytical chemistry*, 79 12, 4463-70

Ross, S. T., Schwartz, S., Fellers, T. J., & Davidson, M. W. (n.d.). Total internal reflection fluorescence (TIRF) microscopy. Nikon's MicroscopyU. Retrieved November 18, 2021, from <https://www.microscopyu.com/techniques/fluorescence/total-internal-reflection-fluorescence-tirf-microscopy>

Einstein, A. (1905), Über die von der molekularkinetischen Theorie der Wärme geforderte Bewegung von in ruhenden Flüssigkeiten suspendierten Teilchen. Ann. Phys., 322: 549-560.  
<https://doi.org/10.1002/andp.19053220806>

Spring, K. R., Davidson, M. W., (n.d.). Introduction to Fluorescence Microscopy. Nikon's MicroscopyU. Retrieved online April 11, 2022, from  
<https://www.microscopyu.com/techniques/fluorescence/introduction-to-fluorescence-microscopy>

Crank, J. (1975), The Mathematics of Diffusion. Brunel University Uxbridge, Clarendon press, Oxford. Can be accessed online: [http://www-eng.lbl.gov/~shuman/NEXT/MATERIALS&COMPONENTS/Xe\\_damage/Crank-The-Mathematics-of-Diffusion.pdf](http://www-eng.lbl.gov/~shuman/NEXT/MATERIALS&COMPONENTS/Xe_damage/Crank-The-Mathematics-of-Diffusion.pdf)

ThermoFisher (n.d.). FluoSpheres™ Carboxylate-Modified Microspheres, 0.1 µm, yellow-green fluorescent (505/515), 2% solids. Retrieved online April 11, 2022.  
<https://www.thermofisher.com/order/catalog/product/F8803>

## Appendix: Software screenshots

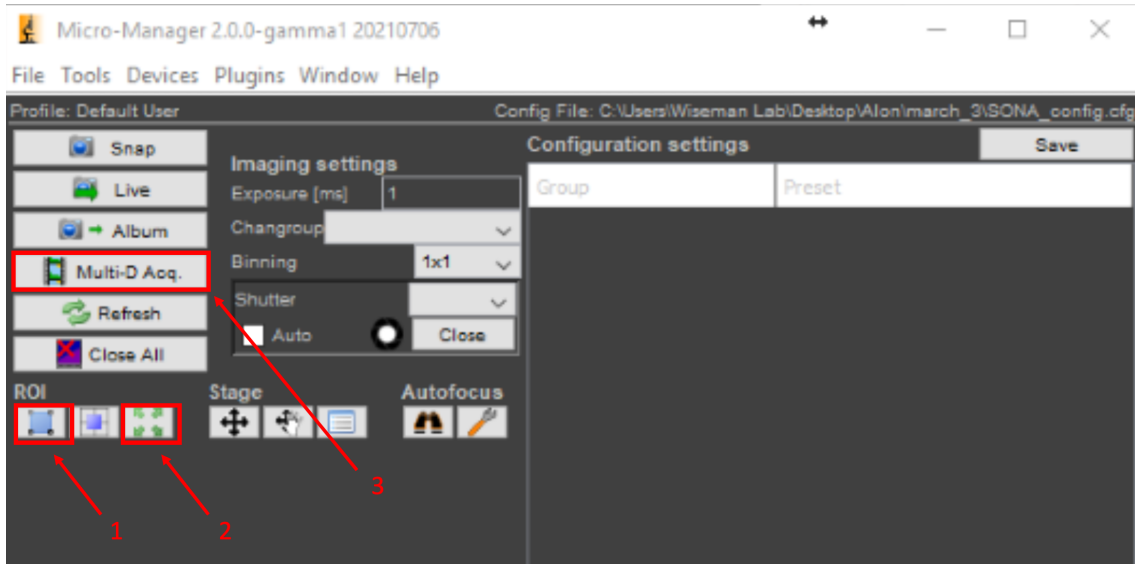


Figure A1. Micro-Manager 2.0 main window. Arrow 1 points to the ROI selection button. Arrow 2 points to the re-setting ROI to maximal size button. Arrow 3 points to the button that opens the movie capturing window. The exposure of the camera can be set in the middle of the window.

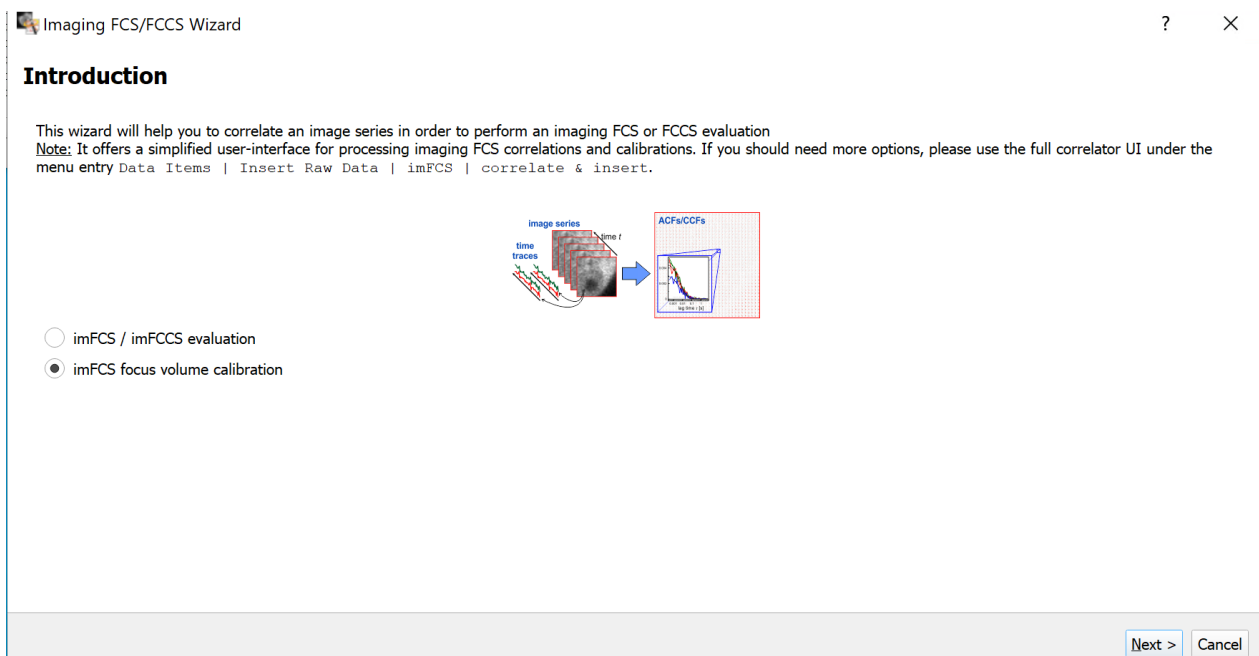


Figure A2. First window of the imaging FCS/FCCS wizard. For image analysis (normal ACF fitting to get concentration and diffusion coefficients) the 'imFCS / imFCCS evaluation' option should be chosen. For the PSF calibration, 'imFCS focus volume calibration' should be chosen.

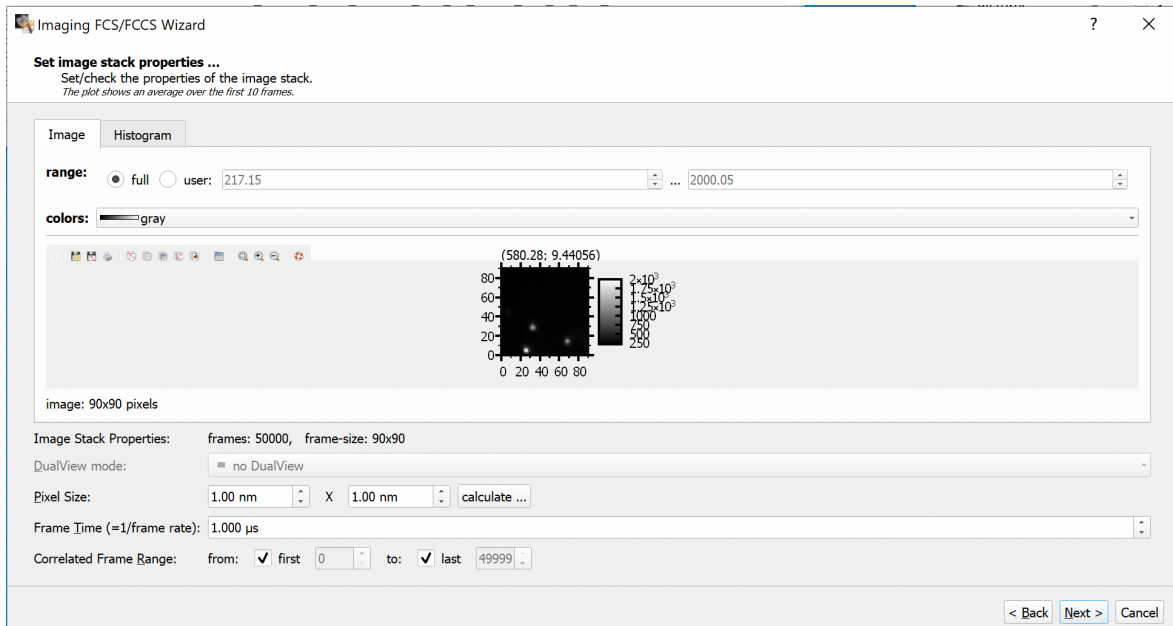


Figure A3. The 'image stack properties' window of the wizard. The loaded image should be verified here. To set the correct pixel size, click on the 'calculate ...' button and input the correct values for the camera that was used. The frame time is the inverse of the frame rate in microseconds.

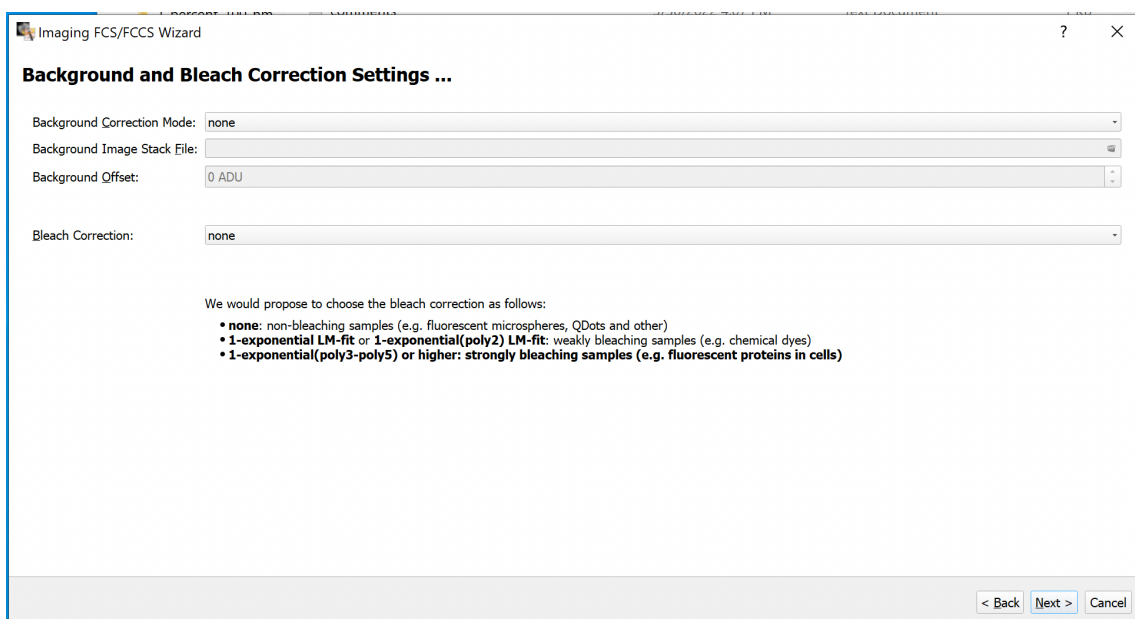


Figure A4. The 'background and bleach correction settings' window of the wizard. If background images were taken, those can be added in this window. Bleach correction should only be used for lipid images.

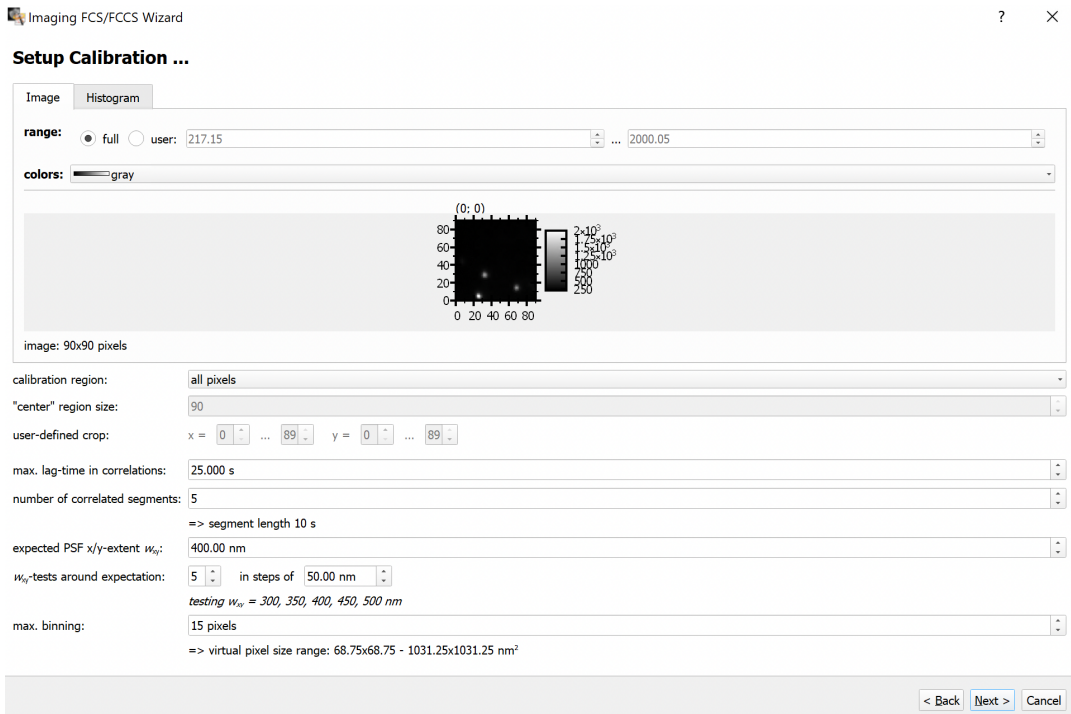


Figure A5. The 'setup calibration' window of the wizard. It is recommended to keep the max. lag-time and the number of correlated segments as the default. The expected true PSF value should be set, with at least 5 guesses distributed around it, at steps of around 50 nm. The maximal binning size should also be set here.

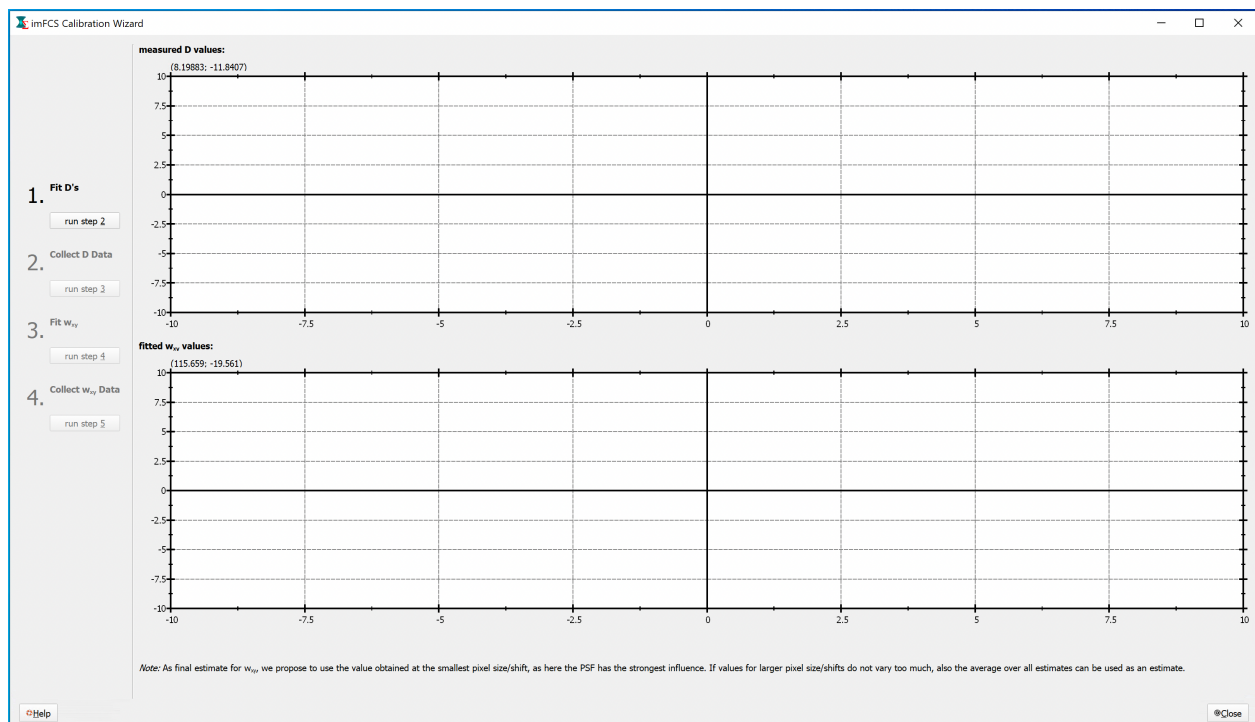


Figure A6. The 'calibration' window of the wizard. The first two buttons will automatically perform the first step of the calibration (ACF fitting with various PSF values, and plotting diffusion coefficient vs. pixel size plot), and the second two buttons will automatically perform the second step of the calibration (ACF re-fitting with the determined reference diffusion coefficient and plotting PSF vs. pixel size).

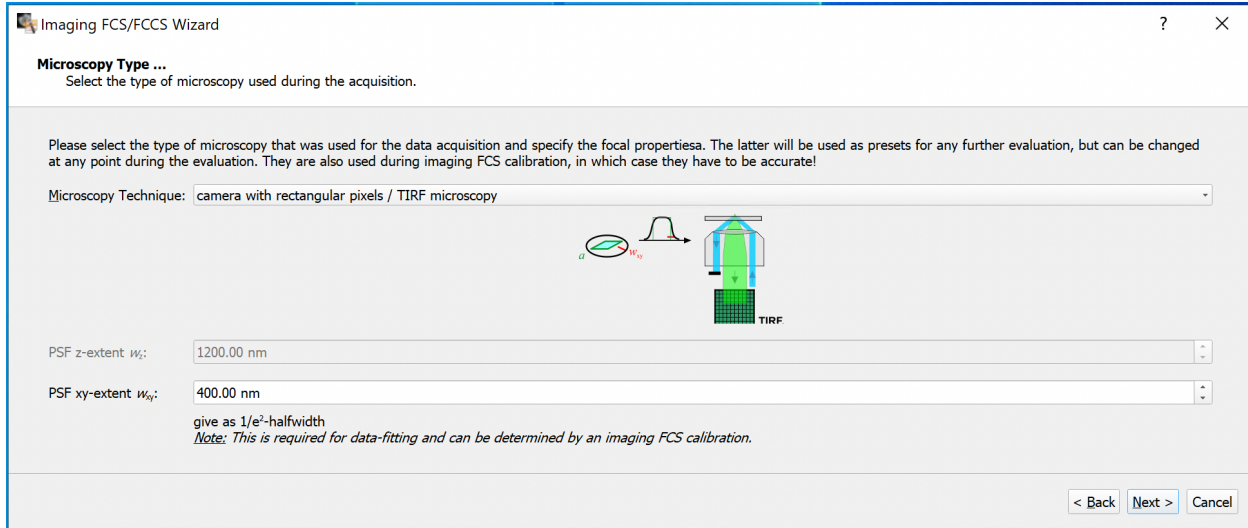


Figure A7. The 'microscope type' window of the ACF fitting wizard. For TIRF images, make sure 'TIRF microscopy' is chosen in the top option, and the correct PSF value is inputted.

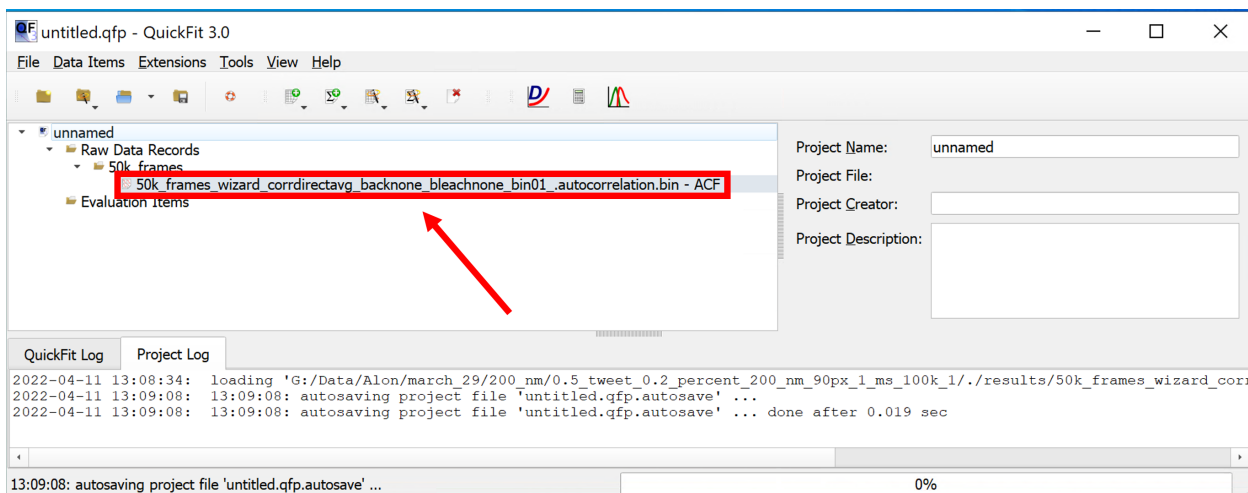


Figure A8. The QF main window after the ACF calculation wizard was used. The arrow is pointing to the file that holds the calculated ACF's. Double clicking it will open the ACF window, where the results can be evaluated.

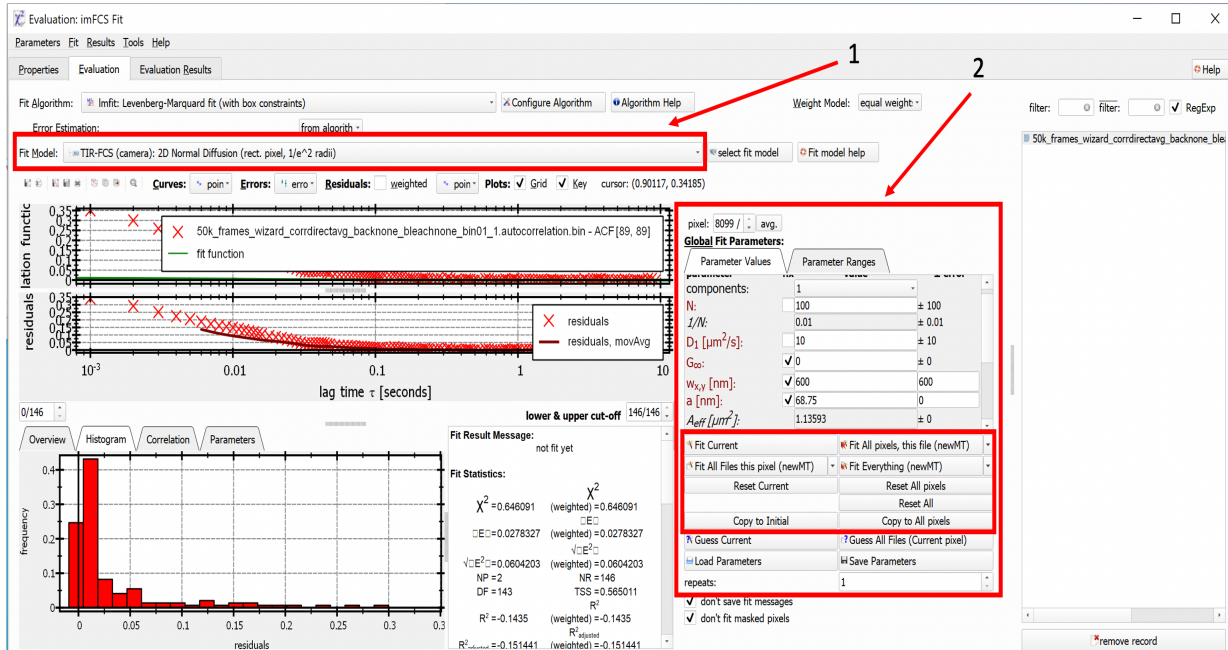


Figure A9. The 'imFCS Fit' window. The ACF function can now be fitted to the data. Choose the appropriate fit model in the option pointed to by arrow 1 ('TIR-FCS (camera): 2D Normal Diffusion' should be chosen for a normal TIRF movie). Arrow 2 is pointing to the fitting menu. Click on 'Fit Current' to fit ACF to the current pixel. The fit can be evaluated by looking at the calculated diffusion coefficient  $D_1$ . A different pixel might be chosen to produce a better fit. Once the fit for the individual pixel is satisfactory, clicking 'Copy to Initial' will copy all the fit parameters to the fitting initial guess, and then 'Fit All pixels, this file' will use those initial guesses to fit all the pixels in the file.

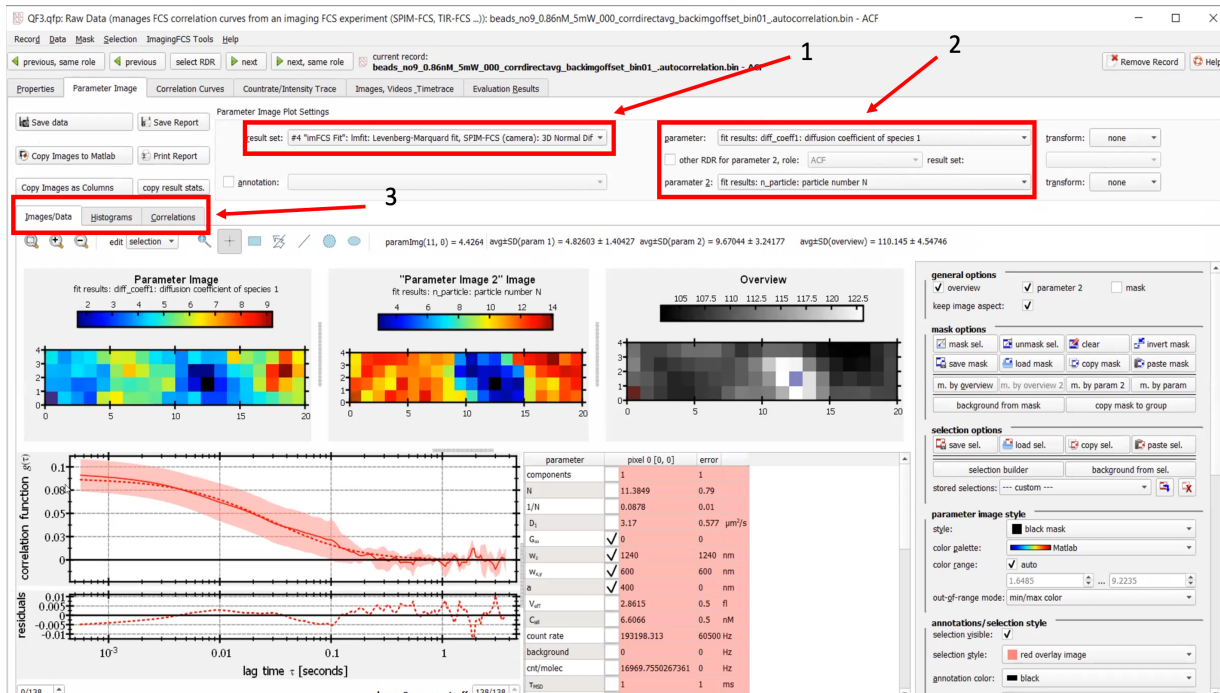


Figure A10. The ACF fit evaluation window. Choose the correct fit result in arrow 1 option. The desired parameters can be selected for evaluation in the arrow 2 drop down menus. Parameter maps and statistics can be evaluated in this window. Histograms for the parameters can be viewed in the 'Histogram' tab in the arrow 3 box.